Journal of Pharmaceutical Sciences 109 (2020) 750-760

Contents lists available at ScienceDirect

Journal of Pharmaceutical Sciences

journal homepage: www.jpharmsci.org

Pharmaceutical Biotechnology

Activation of Human Monocytes by Colloidal Aluminum Salts

Hilde Vrieling [1, 2], Sietske Kooijman [1, 3], Justin W. de Ridder [1], Dominique M.E. Thies-Weesie [4], Peter C. Soema [1], Wim Jiskoot [2], Elly van Riet [1], Albert J.R. Heck [3, 5], Albert P. Philipse [4], Gideon F.A. Kersten [1, 2], Hugo D. Meiring [1], Jeroen L. Pennings [6], Bernard Metz [1, *]

[1] Intravacc (Institute for Translational Vaccinology), Bilthoven, the Netherlands
[2] Division of BioTherapeutics, Leiden Academic Centre for Drug Research (LACDR), Leiden University, Leiden, the Netherlands
[3] Biomolecular Mass Spectrometry and Proteomics, Bijvoet Center for Biomolecular Research and Utrecht Institute for Pharmaceutical Sciences, Science Faculty, Utrecht University, Utrecht, the Netherlands
[4] Van 't Hoff Laboratory for Physical and Colloid Chemistry, Debye Institute for Nanomaterials Science, Utrecht University, Utrecht, the Netherlands
[5] Netherlands Proteomics Centre, Utrecht, the Netherlands
[6] Centre for Health Protection, National Institute for Public Health and the Environment (RIVM), Bilthoven, the Netherlands

ARTICLE INFO

Article history:
Received 18 April 2019
Revised 10 August 2019
Accepted 15 August 2019
Available online 23 August 2019

Keywords:
alum
aluminum hydroxide
colloids
immune responses
proteomic
vaccine adjuvants

ABSTRACT

Subunit vaccines often contain colloidal aluminum salt–based adjuvants to activate the innate immune system. These aluminum salts consist of micrometer-sized aggregates. It is well-known that particle size affects the adjuvant effect of particulate adjuvants. In this study, the activation of human monocytes by hexagonal-shaped gibbsite (ø = 210 ± 40 nm) and rod-shaped boehmite (ø = 83 ± 827 nm) was compared with classical aluminum oxyhydroxide adjuvant (alum). To this end, human primary monocytes were cultured in the presence of alum, gibbsite, or boehmite. The transcriptome and proteome of the monocytes were investigated by using quantitative polymerase chain reaction and mass spectrometry. Human monocytic THP-1 cells were used to investigate the effect of the particles on cellular maturation, differentiation, activation, and cytokine secretion, as measured by flow cytometry and enzyme-linked immunosorbent assay. Each particle type resulted in a specific gene expression profile. IL-1ß and IL-6 secretion was significantly upregulated by boehmite and alum. Of the 7 surface markers investigated, only CD80 was significantly upregulated by alum and none by gibbsite or boehmite. Gibbsite hardly activated the monocytes. Boehmite activated human primary monocytes equally to alum, but induced a much milder stress-related response. Therefore, boehmite was identified as a promising adjuvant candidate.

Introduction

Many prophylactic vaccines contain colloidal aluminum salt-based adjuvants, which enhance the immune response after vaccination. Colloidal aluminum salt-based adjuvants promote the activation and maturation of antigen-presenting cells (APCs), which have a key role in the activation of the adaptive immune system.[1] Traditionally, these adjuvants consist of aluminum salts that form aggregates of 0.5-10 μm on dispersion in water.[2] However, nanoparticles can also be formed of aluminum salts and may be favorable compared to the traditional adjuvants.[3,4] For example, the antigen-specific antibody response in mice was stronger when adsorbing ovalbumin and *Bacillus anthracis* antigens to nanoparticles of aluminum hydroxide than when adsorbing the antigens to microparticles.[5] In addition, the size of aluminum oxyhydroxide nanorods was positively related to the adaptive humoral immune response when using ovalbumin as model antigen. Moreover, aluminum (oxy)hydroxide nanoparticles induced higher levels of uric acid compared to microparticles both *in vitro* and *in vivo*.[6] Besides particle size, particle shape may affect the immune-stimulating properties of particulate adjuvants.[7] For instance, rod-shaped nanoparticles were more potent adjuvants compared to plates and polyhedra.[8] Thus, aluminum salt-based based nanoparticles may have stronger adjuvant effect than aluminum salt-based microparticles.

Conflict of interest: None.
The authors Hilde Vrieling and Sietske Kooijman contributed equally.
This article contains supplementary material available from the authors by request or via the Internet at https://doi.org/10.1016/j.xphs.2019.08.014.
* *Correspondence to:* Bernard Metz (Telephone: +31 30 7920 485).
E-mail address: bernard.metz@intravacc.nl (B. Metz).

https://doi.org/10.1016/j.xphs.2019.08.014

Most studies address the immune response against an antigen formulated with aluminum salt-based particles. However, little is known about the intrinsic capacity of these particles to activate the innate immune system. Monocytes play an important role in the onset of an immune response.[9,10] The activation of monocytes induced by adjuvants can be studied by analyzing the protein and gene expression. For example, the secretome of human monocytes incubated *in vitro* with Adju-Phos®, monophosphoryl lipid A or R848 in absence of an antigen was studied with mass spectrometry.[11] In the same study, incubation of monocytes with complete vaccines, that is, formulations containing antigen, was investigated. Each adjuvant induced a distinct secretome profile in monocytes. The response to vaccines (antigen and adjuvant) was similar to the response to the adjuvants alone. In addition, molecular responses of MF59, CpG, and aluminum hydroxide have been analyzed at the site of injection in murine muscle cells without the presence of an antigen.[12] All adjuvants modulated the gene cluster "adjuvant core response gene," resulting in upregulation of gene expression of cytokines, chemokines, and adhesion molecules. Local responses were activated the most by MF59, as demonstrated by increased expression of genes encoding proinflammatory cytokines. CpG induced the strongest systemic responses as demonstrated by increased cytokine concentrations in sera.[12] Transcriptome and proteome analyses may thus help to unravel the molecular mechanisms of adjuvants.

In this study, the effects of 2 experimental colloidal aluminum salts, that is, gibbsite (aluminum hydroxide) and boehmite (aluminum oxyhydroxide), on the activation and response of human monocytes was studied. These colloidal aluminum salts may be suitable vaccine adjuvant. Besides chemical differences, gibbsite and boehmite also differ in the specific surface area. Gibbsite has a relatively low specific surface area of 76 m^2/g as compared to boehmite (514 m^2/g).[13,14] To investigate the effect of colloidal aluminum salt–based adjuvants on the activation of human monocytes, we used a multiomics approach, by analyzing both protein and mRNA expression profiles in adjuvant-exposed human monocytes. Human monocytes have been shown to be a suitable *in vitro* model for this purpose.[1] The *in vitro* cellular responses caused by gibbsite and boehmite were compared to those induced by a commercially available micrometer-sized aluminum oxyhydroxide adjuvant, further referred to as alum, which consists of aggregated rod-shaped nanoparticles with average dimensions of $4.5 \times 2.2 \times 10$ nm.[15] The collective results demonstrate that gibbsite, boehmite, and alum differently activate human monocytes, which are involved in the induction of the innate immune response.

Materials and Methods

Materials

Alum (Alhydrogel® 2%, batch 5240) was purchased from Brenntag Biosector (Frederikssund, Denmark). Aluminum-iso-propoxide and aluminum-*sec*-butoxide were purchased from Sigma-Aldrich.

Synthesis of Gibbsite and Boehmite

Gibbsite and boehmite were synthesized as described previously.[14,16,17] Briefly, 80 mM aluminum-iso-propoxide was mixed with 80 mM aluminum-*sec*-butoxide in 90 mM HCl in water. The solution was stirred for 10 days. After hydrothermal treatment at 150°C (boehmite nanoparticles) or 85°C (gibbsite nanoparticles) for 36 h, the suspension was dialyzed against ultrapure water (Milli-Q, resistivity = 18.2 MΩ.cm, total organic carbon <5 ppb) using dialysis cassettes with a cutoff of 10 kDa for at least 14 days. During this procedure, the dialysate was replaced at least 8 times. Suspensions were autoclaved and stored at room temperature. Autoclaving had no effects on particle shape, size, and charge (data not shown).

The quantification of Al^{3+} ions in gibbsite and boehmite was performed using a colorimetric assay. Standards were prepared by diluting 150 μM $AlCl_3$ in 6 M KOH, so that the final range of the calibration line was 0-15 μM Al^{3+}. Samples were also diluted in 6 M KOH so that the maximum concentration Al^{3+} was not higher than 0.85 mM. Samples and standards were heated at 100°C for 60 min to dissolve aluminum salts. After cooling to room temperature, standards, and samples were diluted in 1 M sodium acetate buffer pH 5.5 to an expected final concentration between 0.1 and 8.5 nM Al^{3+}. Fifty μL of each sample or standard was added to a transparent polystyrene flat-bottom 96-wells plate (Greiner Bio-One) in triplicate. To each well, 50 μL of 12 mM dodecyltrimethylammonium bromide, 50 μL of 600 μM eriochrome cyanide R and 50 μL of 1 M sodium acetate buffer pH 5.5 was added. The plate was incubated on a plate shaker at 600 rpm at RT for 15 min. The absorbance was determined at 584 nm by using a SynergyMx reader (BioTek). Aluminum concentrations in samples were calculated to be 6.0 mg Al^{3+}/mL for gibbsite and 3.1 mg Al^{3+}/mL for boehmite based on the standard curve using Gentech 5 software (BioTek).

Transmission Electron Microscopy

Transmission electron microscopy (TEM) was performed by using a Philips Tecnai 10 electron microscope, typically operating at 100 kV. The samples were prepared by drying a drop of diluted, aqueous particle dispersion on top of polymer-coated copper grids. For gibbsite and boehmite, the dimensions of at least 100 particles were determined with AnalySIS Pro imaging software. Both the number-averaged length and width and standard deviations of boehmite were measured. The diameter and standard deviation of gibbsite were calculated by averaging the measurements of the 3 opposing corners per particle.

Dynamic Light Scattering

The hydrodynamic diameter was measured by dynamic light scattering using a Zetasizer Nano ZS (Malvern Instruments Ltd.). Sixty μL of each sample containing 125 μg/mL Al^{3+} (alum), 750 μg/mL Al^{3+} (gibbsite) or 386 μg/mL Al^{3+} (boehmite) in 1 mM NaCl or in cell culture medium, was measured in single-use polystyrene UV micro cuvettes (BRAND®). The Dispersion Technology Software (version 7.11) was used for collection and analysis of the data. Each sample was measured at 25°C in triplicate with an automatic attenuator. The number of runs and the measurement duration were automatically optimized by the software.

Laser-Doppler Electrophoresis

The electrophoretic mobility was measured by using a Zetasizer Nano ZS. Folded capillary cells (DTS1070; Malvern Instruments Ltd.) were filled with 800 μL sample containing 1.2 mg/mL Al^{3+} diluted in 1 mM NaCl or in cell culture medium. The Dispersion Technology Software (version 7.11) was used for collection and analysis of the data. Zeta potential values were calculated according to the Smoluchowski equation. Each sample was measured at 25°C in triplicate with an automatic attenuator. The number of runs and the measurement duration were automatically optimized by the software.

Culture of Primary Monocytes

The human monocyte study was conducted according to the principles expressed in the Declaration of Helsinki. All blood donors gave written-informed consent before collection and use of their

samples. All blood donations, provided by the Dutch National Institute for Public Health and the Environment (RIVM, Bilthoven, the Netherlands) were specifically donated for primary cell isolation. This research goal was explicitly approved by the accredited Medical Ethical Committee (Medisch Ethische Toetsingscommissie), Noord-Holland in the Netherlands. All blood samples were processed anonymously.

Fresh peripheral blood was collected from healthy volunteers and collected in heparin-coated tubes. Peripheral blood mononuclear cells (PBMCs) were isolated from whole blood using Ficoll® density centrifugation at 1000 × *g* for 30 min. Monocytes were isolated by positive selection using CD14 microbeads and a magnetic LS MACS column (Miltenyi Biotech). Monocytes (>95% purity) were cultured at 400,000 cells/well in 24-wells plates in cell culture medium (Roswell Park Memorial Institute Media 1640 (RPMI) containing 10% (v/v) fetal calf serum (Serana), 100 units/mL penicillin, 100 μg/mL streptomycin and 0.3 μg/mL L-glutamine) in the presence of alum, gibbsite or boehmite (each at a concentration of 10 μg/mL Al^{3+}) or were left unstimulated for 6, 24, or 48 h.

Cell viability was determined by flow cytometry. To this end, primary monocytes were washed twice with fluorescence-activated cell sorting (FACS) buffer (0.5% (w/v) bovine serum albumin and 0.5 mM ethylenediaminetetraacetic acid in phosphate-buffered saline [PBS, 1.06 mM KH_2PO_4, 155 mM NaCl, 2.97 mM Na_2HPO_4, pH 7.2]) by centrifugation at 300 × *g* for 3 min. After centrifugation, pellets were resuspended in 100 μL FACS buffer containing fixable viability stain 780 in a 1:2000 dilution. Cells were incubated at 4°C for 30 min. After staining, cells were washed with FACS buffer and resuspended in 150 μL FACS buffer. Cell populations were analyzed by flow cytometry using Attune NxT (ThermoFisher Scientific). Attune™ NxT Software V2.6 was used for data collection. Samples were analyzed by using FlowJo software, version 10.2 (Treestar).

Culture of THP-1 Cells

Human THP-1 cells were grown in cell culture medium at 37°C with 5% CO_2. Cells were primed overnight with 300 ng/mL phorbol myristate acetate (InvivoGen) in a 96-wells plate containing 100,000 cells/well in a total volume of 200 μL/well. After priming, cells were washed 3 times with cell culture medium by centrifugation at 300 × *g* for 5 min. The supernatant was discarded and alum, gibbsite, or boehmite was added at a final concentration of 0.1 mg/mL Al^{3+} in the presence of 2.5 ng/mL LPS in culture medium in a total volume of 200 μL/well. LPS was also added to the control wells. Cells were incubated at 37°C with 5% CO_2 for 24 h and centrifuged at 300 × *g* for 5 min. Supernatants (170 μL/well) were stored at −20°C until further use. Cells were immediately processed for surface marker analysis. To this end, monocytes were washed twice with FACS buffer by centrifugation at 300 × *g* for 3 min. After centrifugation, pellets were resuspended in 100 μL FACS buffer containing antibody-fluorochrome conjugates CD83-APC (HB15E), CD40-BV711 (5C3), CD86-BV510 (FUN-1), CD14-PE (H5E2), CD11c-BV421 (B-ly6/3.9), CD80-BB515 (L307.4), or HLA-DR-PerCP (L243) in a 1:20 dilution and fixable viability stain 780 in a 1:2000 dilution. Cells were incubated at 4°C for 30 min. After staining, cells were washed with FACS buffer and resuspended in 150 μL FACS buffer. Cell populations were analyzed by flow cytometry using Attune NxT (ThermoFisher Scientific). Attune™ NxT Software V2.6 was used for data collection. Samples were analyzed by using FlowJo software, version 10.2 (Treestar). The gating strategy can be observed in Supplementary Figure S1.

Cytokine Secretion

Cytokine (IL-1ß [Ready-SET-Go!, e Bioscience], IL-4, IL-6, IL-10, IL-17A [uncoated kits, all from Thermo Fisher Scientific] and IL-18 [matched antibody pair, Thermo fisher Scientific]) concentrations were measured in the culture supernatants of primary monocytes and THP-1 cells by using ELISA kits according to the manufacturer's instructions. The light absorbance was determined at 450 nm by using a SynergyMx reader (BioTek). Cytokine concentrations in samples were calculated based on the standard curves by using Gentech 5 software (BioTek).

mRNA Expression

The levels of mRNA expressed by 89 genes which are involved in innate and adaptive immunity and 7 controls were determined. Monocytes were lysed with RLT buffer (Qiagen). Subsequently, mRNA was extracted using the RNeasy mini kit (Qiagen), according to the manufacturer's animal cell spin protocol. RNA purity and concentration were determined on a SynergyMX (BioTek) plate reader (UV 260 nm and 280 nm). Depending on the amount of mRNA available, 10 or 12 ng of cDNA was synthesized. Each sample was normalized to an unstimulated control with the same amount of cDNA. The cDNA was synthesized by using the RT cDNA synthesis kit and the RT preAMP Pathway primer mix "Innate and Adaptive immunity" (Qiagen) according to the manufacturer's protocol. cDNA was stored at −20°C.

Subsequently, quantitative polymerase chain reaction analysis (Roche light cycler 96) was performed with "Innate and Adaptive Immune response RT2 profiler arrays" (Qiagen), comprising 84 functional genes, 5 housekeeping genes and 7 controls, both positive and negative, for determining the reliability of the experiments. A melt curve determination was performed as quality control for binding of the primer to the sample.

The polymerase chain reaction array contained 5 housekeeping genes (ACTB, B2M, GAPDH, HPRT1, and RPLP0). The 4 most stable housekeeping genes were used in the calculations (B2M, GAPDH, HPRT1, and RPLP0 after 6 h of incubation; ACTB, B2M, HPRT1, and RPLP0 after 24 h of incubation). The Ct values, representing the number of cycles that was needed to obtain a fluorescence above that of the threshold, of these 4 genes were averaged resulting in a general housekeeping gene value. This general housekeeping gene value was used for normalization of the target gene expression value of each gene, which is expressed as ΔCt. Target gene expressions of stimulated monocytes were normalized to unstimulated control and is expressed as ΔΔCt (Supplementary Table S2). Expression changes for 3 donors were compared and genes that showed a twofold increase or decrease in at least 2 of 3 biological replicates were considered differentially expressed. For these genes the median values across the 3 biological replicates were visualized as a heatmap combined with hierarchical clustering (Euclidean distance, Ward.D linkage) by using R statistical software (version 3.4.0).

Isolation, Digestion, and Labeling of Proteins

Cells were centrifuged at 300 × *g* for 5 min and washed twice with 500 μL of ice-cold PBS. Cell lysis, total protein analysis, and digestion were performed as described previously.[1,18]

Of the digested protein samples from the 8 incubation conditions per donor (culture medium, alum, gibbsite, and boehmite, each after 24 and 48 h of incubation), the protein content was normalized and diluted in 100 mM phosphate buffer pH 7.5. Samples were desalted by using C18 Solid Phase Extraction (Waters) according to the manufacturer's protocol and dried by centrifugation under reduced pressure. The samples were labeled per condition by using tandem mass tag labeling-10plex (TMT(10)), (Thermo Fisher Scientific), pooled and dried by centrifugation under reduced pressure. Subsequently, samples were dissolved in ultrapure water with 5% (v/v) DMSO and 0.1% (v/v) formic acid for proteome analysis.

Liquid Chromatography—Mass Spectrometry Analysis

Peptide separation by reversed phase liquid chromatography—mass spectrometry and tandem mass spectrometry was performed on an Agilent 1290 Infinity system (Santa Clara). Peptides were trapped on a fritted trapping reversed-phase chromatography column Reprosil-Pur C18-AQ, df = 5 μm, 2 cm L × 100 μm I.D. (Dr. Maisch), made in-house and separated on an in-house packed reversed-phase analytical column (Reprosil-Pur C18-AQ, df = 3 μm, 30 cm L × 50 μm I.D., Dr. Maisch). Solvent A was 0.1% (v/v) formic acid in ultrapure water and solvent B was 0.1% (v/v) formic acid in acetonitrile (Biosolve). The peptides were separated in 195 min at a column flow rate of 125 nL/min in a nonlinear gradient (15 min at 0% B, a gradient of 160 min from 0% to 30% B, a 15 min gradient to 45% B and 5 min at 65% B) optimized as described by Moruz et al.[19] The column effluent was electrosprayed directly into the mass spectrometer by using a gold-coated fused silica tip of 3.5-μm, with a spray voltage of 2.1 kV.

Mass spectrometric data were acquired on a Tribrid-Orbitrap Fusion Lumos (Thermo Fisher Scientific). The full scan (MS1) spectra were acquired with a scan mass range of 350-1500 m/z at 120,000 resolution (FWHM) with an Orbitrap readout. For the MS1, the automatic gain control (AGC) was set to 400,000 and the maximum injection time was 50 ms. Top speed mode was chosen with a duration of 3 s where precursor ions with an intensity >5000 were selected for fragmentation (MS2). Charge states between 2 and 7 were selected for MS2, which was performed by using collision-induced dissociation in the linear ion trap with a normalized collision energy of 35%. In MS2, the AGC was set to 10,000 and the maximum injection time was 100 ms. Synchronous precursor selection was enabled to include up to 5 MS2 fragment ions for MS3. These fragment ions were further fragmented by higher energy collision dissociation with a normalized collision energy of 60%. The TMT reporter ions were analyzed in the Orbitrap analyzer, the AGC was set to 100,000 and the maximum injection time was set to 240 ms.

Proteomics data were analyzed with Proteome Discoverer 2.1 (Thermo Fisher Scientific); unless stated otherwise, default settings were used. Precursor mass tolerance was set to 5 ppm. MS2 scans were searched against the human UniProt database of November 2014, containing 23,048 entries, by using the Sequest HT search engine with a full enzyme specificity for Lys-C as described previously.[1] The quantification node was used to obtain relative expression values, where TMT(10) was defined as the quantification method, with an integration tolerance of 0.2 Da. Cite Percolator was used to filter the peptide-to-spectrum mass with a false discovery rate of <5%. Next, data were normalized by performing a median correction. Data of 3 biological replicates were compared, proteins that were upregulated or downregulated by 1.5-fold or more compared to control, in at least 2 of 3 replicates were considered significantly regulated as described previously.[1] The regulated proteins were imported in STRING (string.embl.de) to identify enriched pathways (false discovery rate<0.05) within functional annotations provided by Gene Ontology biological processes and Kyoto Encyclopedia of Genes and Genomes pathways.

Results

Particle Characterization

The effects of aluminum salt—based particles on monocytes were investigated by using 2 experimental aluminum salts, that is, gibbsite and boehmite, and alum. Primary particles of alum and boehmite are rod-shaped, whereas gibbsite consisted of hexagonal nanoparticles, as confirmed by TEM analysis (Fig. 1). Primary rod-shaped particles of alum form aggregates of 2-12 μm.[20] According

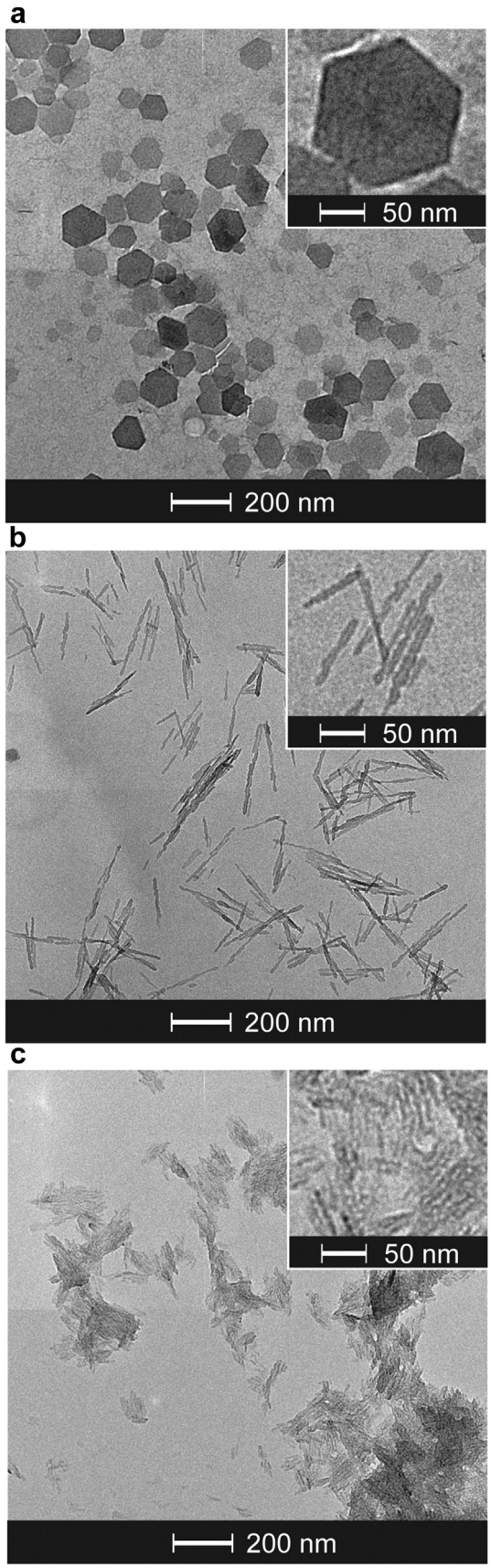

Figure 1. Representative TEM images of gibbsite nanoparticles (a), boehmite nanoparticles (b), and alum (c). The inserted images show a more detailed shape of the particles.

to TEM analysis, individual gibbsite particles had an average diameter of 210 ± 40 nm, whereas individual boehmite rods had a length of 83 ± 27 nm and a width of 22 ± 3 nm. The 3 aluminum salts were dispersed in ultrapure water to estimate the aggregation of the primary particles on dispersion. Components that are present during cell culture, such as salts and proteins, may influence the size and zeta potential of the particles. Therefore, the 3 aluminum salts were also dispersed in culture medium. In ultrapure water, alum consisted of particles with a hydrodynamic diameter of 744 ± 5 nm and a polydispersity index (PdI) of 0.162 ± 0.074. The hydrodynamic diameter of dispersed gibbsite and boehmite was 155 ± 2 and 502 ± 13 nm with a PdI of 0.085 ± 0.023 and 0.234 ± 0.017, respectively (Table 1). The hydrodynamic diameter of gibbsite and boehmite increased to 1467 ± 188 and 1110 ± 120 nm with a corresponding PdI of 0.564 ± 0.046 and 0.427 ± 0.083, respectively (Table 1). The hydrodynamic diameter of alum decreased to 583 ± 5 with a corresponding PdI of 0.72 ± 0.037 in culture medium. The zeta potential of the 3 aluminum salt-based particles in ultrapure water varied from 12 to 53 mV (Table 1). The zeta potential of all types of particles was reduced to −9 mV on dispersion in culture medium. This can be attributed to the presence of salts and proteins in the culture medium, altering the ionic strength of the dispersion and potentially leading to protein adsorption to the particles.

Gene Expression

Human primary monocytes were incubated with each of the aluminum salts. Cell viability was not affected by any of the colloidal aluminum salts (data not shown). The effects on expression of 89 genes related to the innate and adaptive immune response were assessed after 6 and 24 h of incubation. After 6 h, monocytes incubated with alum showed altered expression of 34 genes. Of these genes, 32 genes were upregulated and 2 genes were downregulated (Supplementary Table S1). Incubation with gibbsite or boehmite affected smaller numbers of genes. Gibbsite altered the expression of 14 genes (13 up and 1 down) and boehmite altered the expression of 9 genes (8 up and 1 down) (Fig. 2a and Supplementary Table S1). Incubation with each of the 3 aluminum salts increased the expression of *IFNα* and *IFNβ* (both proinflammatory cytokines), *APCS* (an acute phase-related gene), and *IL-4* (a Th2-polarizing cytokine) (Fig. 2a). Alum increased the gene expression of *HLA-A*, *IL-2*, *IL-6*, and *IL-17A* (the latter 3 are proinflammatory cytokines) and the cell surface marker *CD8A* (related to an inflammatory response and coactivation of FcγR).[21] Incubation of monocytes with gibbsite induced increased mRNA levels of *CD4* (associated with the differentiation to functional macrophages)[22] and *TICAM1* (involved in TLR-mediated interferon regulatory factor signaling). Both gibbsite and alum induced upregulation of expression of several genes, including *IL-5* (Th2 signatory cytokine) and *IFNγ* (Th1 signatory cytokine) (Fig. 2a). Boehmite activated *CSF2* (related to the proliferation of monocyte-derived proinflammatory macrophages)[23] and *CCR6* (a receptor for CCL20, present on dendritic cells [DCs] and effector/memory B and T cells). Based on these data, the gene expression profiles of alum and gibbsite showed both monocytic activation toward a Th2-polarizing response by inducing expression of *IL-4* and a Th1-polarizing response by inducing *IFNγ*. Boehmite did not induce expression of the Th1-associated gene IFNγ. Altogether, the activation of monocytes that was induced by gibbsite and boehmite was less pronounced than that induced by alum.

The gene expression profiles of the monocytes were also determined after 24 h of incubation with gibbsite, boehmite or alum. All 3 colloidal aluminum salts increased the gene expression of among others *CCR8* (a chemokine receptor involved in monocyte chemotaxis), *IFNα*, *IL-17A*, *IFNγ*, *IL-1ßL* and *IL-6*. Gene expression levels that were upregulated after 6 h and still being expressed after 24 h included the proinflammatory cytokines *IFNα* (induced by all aluminum salts), *IL-17A* (induced by alum), *IFNγ*, *IL-1ß* and *IL-6* (Fig. 2b, Supplementary Table S1). After 24 h of incubation, incubation with alum, gibbsite, or boehmite caused differential gene expression. *IL-2* (a cytokine involved in natural killer [NK] cell proliferation and required for T cell survival) was upregulated by alum and downregulated by both gibbsite and boehmite (Fig. 2b). On the contrary, *CD14* (a monocyte differentiation marker) was downregulated by alum and upregulated by gibbsite and boehmite. *CD8A* was exclusively upregulated on incubation with alum. The expression of *IL-4* (a cytokine involved in Th2 polarization) was upregulated by alum and downregulated by boehmite. Gibbsite and boehmite induced *NFκB1*, *NFκB1a* (both transcription factors), *STAT4* (involved in regulating the differentiation of T cells), and *TNFα* (a proinflammatory cytokine mainly secreted by macrophages) (Fig. 2b). Incubation with gibbsite increased the gene expression of *CCR5* and its ligand *CCL5* (responsible for attracting monocytes and memory T cells) and of the TLR adapter molecule *TICAM1* more pronounced than incubation with boehmite of alum did. Incubation with boehmite induced the expression of *CXCL10* (an IFNγ-induced transcript and a chemoattractant for monocytes, DCs, and T cells).

At both time points, incubation with gibbsite or boehmite induced the expression of genes related to the differentiation toward macrophages by upregulating *TNFα*, *CSF2*, or CD4. After 6 h of incubation, alum induced the expression of genes related to the differentiation of DCs.

Altogether, all 3 types of colloidal aluminum salts induced the expression of mRNA coding for proinflammatory cytokines. The induction of genes expressing Th2-polarizing cytokines was faster and more pronounced in monocytes incubated with alum than with gibbsite or boehmite. Incubation of monocytes with gibbsite induced expression of similar genes compared to alum. However, both gibbsite and boehmite induced the expression of immune system–related genes to a lesser extent. Based on these gene expression profiles, alum seems to be a more potent innate immune activator than gibbsite and boehmite at the doses tested.

Protein Expression

For a quantitative proteome analysis, monocytes were incubated with alum, gibbsite, or boehmite. The proteome was analyzed after

Table 1
Physicochemical Properties of Aluminum Salts

Compound	Composition	Ultrapure Water			Culture Medium		
		Hydrodynamic Diameter (nm)	PdI	Zeta Potential (mV)	Hydrodynamic Diameter (nm)	PdI	Zeta Potential (mV)
Gibbsite	Aluminum hydroxide	155 ± 2	0.085 ± 0.023	53 ± 1	1467 ± 188	0.564 ± 0.046	−9 ± 0
Boehmite	Aluminum oxyhydroxide	502 ± 13	0.234 ± 0.017	33 ± 1	1110 ± 120	0.427 ± 0.083	−9 ± 1
Alum	Aluminum oxyhydroxide	744 ± 5	0.162 ± 0.074	12 ± 0.3	583 ± 5	0.72 ± 0.037	−9 ± 1

Data are presented as mean ± SD ($n = 3$).

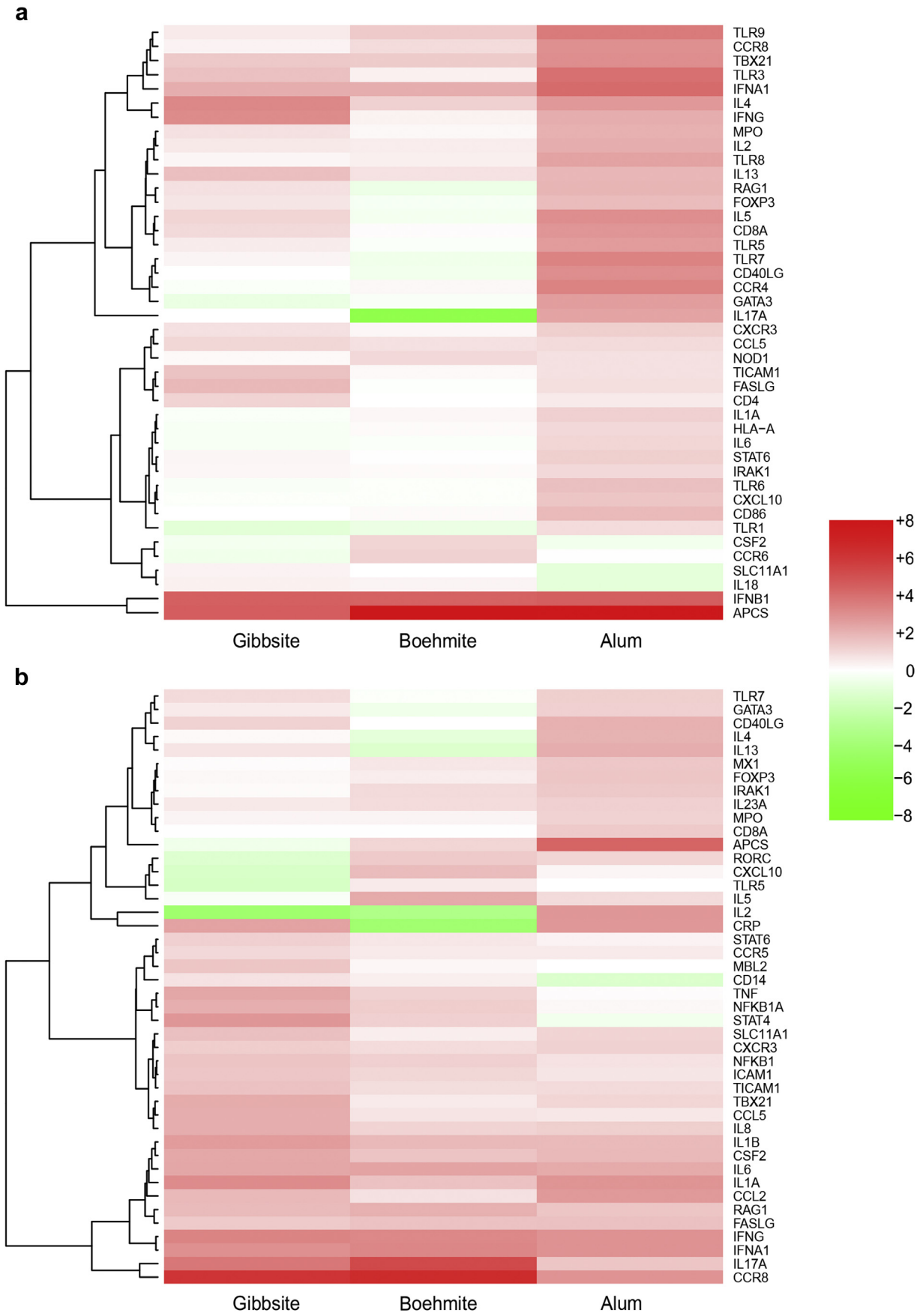

Figure 2. Heatmap of differentially expressed genes by monocytes after incubation with gibbsite nanoparticles, boehmite nanoparticles, or alum. The genes that induced a fold change of 2 or greater in one of the incubation conditions after 6 h (a) or 24 h (b) were clustered by using Euclidean distance. The color bar indicates ΔΔCt values.

24 and 48 h of incubation. The proteome analysis revealed about 1200 quantified proteins in total (Supplementary Table S2). Incubation with alum altered the expression of 72 proteins compared to unstimulated cells, whereas both gibbsite nanoparticles and boehmite nanoparticles resulted in 40 differentially expressed proteins each (Supplementary Table S2). The proteins that were differentially expressed as a result of the incubation with gibbsite were similarly affected by incubation with alum. The protein expression profile of monocytes incubated with boehmite differed at both time points from that of monocytes incubated with alum or gibbsite.

After 24 h of incubation, 2 immune system-related pathways, that is, regulation of the inflammatory response and complement and coagulation cascade, were induced on incubation with alum (Supplementary Table S3). Incubation with gibbsite also resulted in the upregulation of 2 immune system-related pathways (regulation of humoral immune response and complement and coagulation cascade). Incubation with boehmite did not result in a measurable induction of immunological pathways (Fig. 3 and Supplementary Table S3).

After 48 h of incubation with alum, additional homeostatic and immunological pathways were enriched, for example, defense response, antigen processing and presentation, negative regulation of metabolic process, response to stress and secretion. Noteworthy, incubation with alum resulted in induction of positive regulation of type IIa hypersensitivity pathway, whereas none of the other incubation conditions upregulated this pathway (Fig. 3 and Supplementary Table S3). No immunological pathways could be annotated as being induced by gibbsite nanoparticles after 48 h of incubation. Nevertheless, individual proteins that are related to an immune response were upregulated by gibbsite, for example, C4 (involved in complement pathways), CD71 (a monocyte activation marker), cathepsin D (involved in antigen processing and presentation), and LGALS3 (binds IgE and is involved in the innate immune response). After 48 h of incubation with boehmite, relevant immunogenic pathways were induced, for example, immune system process, innate immune response and antigen presentation of exogenous peptide via HLA class I (Fig. 3). These pathways were less enriched with fewer proteins that were significantly expressed compared to those expressed by incubation with alum. Incubation with boehmite resulted in the induction of a limited number of homeostatic pathways with a much lower power compared to alum.

After 24 h of incubation, none of the aluminum salts downregulated pathways compared to unstimulated cells (Fig. 3). After 48 h of incubation, boehmite induced downregulation of complement activation lectin pathway, which is an immunological pathway. Incubation with alum or gibbsite also induced downregulation of pathways, for example, regulation of catabolic process and platelet aggregation. However, these pathways did not belong to immunological pathways. Incubation with alum mainly resulted in downregulation of pathways related to homeostasis, whereas incubation with gibbsite mainly resulted in the downregulation of transport-related pathways (Fig. 3).

In summary, our data strongly suggest that gibbsite and boehmite are less cell activating than alum at the doses tested. Incubation of monocytes with gibbsite resulted in the induction of regulation of humoral immune response after 24 h and no significantly altered pathways after 48 h of incubation. Incubation with boehmite resulted in the induction of immunological pathways after 48 h of incubation, but not after 24 h. Incubation with alum resulted in the induction of pathways related to an immune response after 24 h. This pathway induction was even more pronounced after 48 h.

Cytokine Secretion

The effects of alum, gibbsite, and boehmite on cytokine secretion by human primary monocytes were determined. However, none of the cytokines measured (IL-1ß, IL-4, IL-6, IL-10, IL-17A, and IL-18) could be detected in the culture supernatants. Low extracellular levels may be due to consumption of the cytokines by the cells or to encapsulation of cytokines in extracellular vesicles.[24] Next, we used a human monocytic cell line (THP-1 cells) to study cytokine secretion, which is a suitable model to study monocyte responsiveness.[25] Priming these cells with Phorbol 12-myristate 13-acetate (PMA) induces the production of intracellular pro-IL-1ß, mimicking the first of 2 steps that are needed for activation of the inflammasome.[26] The second step was induced by incubation of THP-1 cells with the different aluminum salts, after which the cytokine concentrations in the supernatants were determined. The viability of the cells was not affected by the aluminum salts (data not shown). Incubation with boehmite nanoparticles or alum induced significantly higher IL-1ß and IL-6 secretion than unstimulated cells (Fig. 4). Incubation with gibbsite did not result in significantly higher IL-1ß or IL-6 levels in the supernatants compared to unstimulated cells. IL-4, IL-10, IL-17A, and IL-18 were not detected in the supernatants of THP-1 cells (data not shown).

Cell Differentiation

The maturation of monocytic THP-1 cells and their differentiation into macrophages or DCs was analyzed by assessing the expression of the surface markers CD11c, CD14, CD40, CD80, CD83, CD86, and HLA-DR. CD14 is highly expressed in monocytes.[27] The level of expression of HLA-DR varies per monocyte subtype.[28] During differentiation into macrophages, the expression of CD14 is downregulated.[29] The surface markers CD40, CD80, CD83, and CD86 are expressed *de novo* during differentiation into mature DCs.[30] The expression of the MHC-II class molecule HLA-DR is increased during differentiation into mature DCs. HLA-DR, CD40, CD80, CD83, and CD86 can be used to analyze subsets of matured DCs.[31] A representative gating strategy is provided in Figure S1. Cells incubated with alum showed a significantly higher percentage of CD80-positive cells compared to unstimulated cells and to cells stimulated with gibbsite or boehmite (Fig. 5). The percentage of positive cells for the other markers was not affected by the stimuli (Fig. S2). Thus, based on the expression of the selected surface markers, no maturation or differentiation of the THP-1 cells was induced by the 3 aluminum salts.

Discussion

In vaccines, the role of an adjuvant is to stimulate and modulate the immune response without causing harmful side effects. Monocytes play an important role in the onset of the immune response.[32] In this study, the influence of 3 aluminum salt—based particles with different size, shape, and composition on the immunological response of human monocytes was investigated *in vitro*. For this purpose, gibbsite (hexagonal-shaped aluminum hydroxide) and boehmite (rod-shaped aluminum oxyhydroxide) were compared to a licensed adjuvant, alum (aluminum oxyhydroxide). Mapping the transcriptome and proteome of human primary monocytes after incubation with alum, gibbsite or boehmite clearly showed distinct differences in gene regulation and activated pathways. Gibbsite and boehmite induced less-intense activation of pathways related to an innate immune response than alum.

Incubation of monocytes with alum induced a more intense proinflammatory activation of monocytes than incubation with

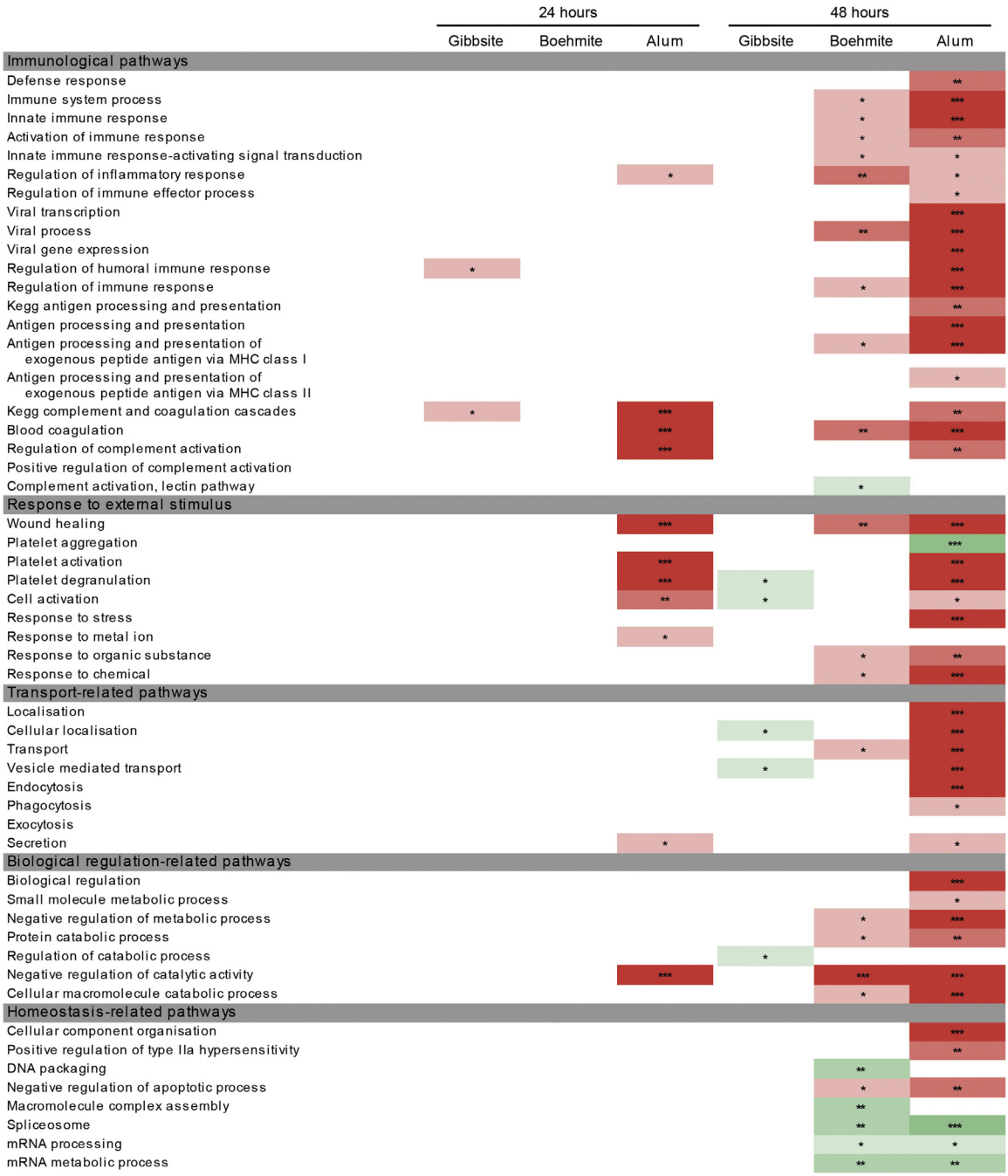

Figure 3. Heatmap view of regulated processes. For each incubation condition, a summary of the enriched pathways is depicted. The pathways are grouped based on immunogenic and homeostatic features. In this heatmap, green and red represent a down and upregulation of gene expression, respectively. The intensity of the color and the asterisks in the cells correspond to the significance of the pathway: * corresponds to a p-value <0.05, ** corresponds to a p-value < 0.01 and *** corresponds to a p-value <0.001.

gibbsite and boehmite. For example, gene expression of *IL-2* (an essential cytokine for T cell survival and NK polarization[33,34]) was upregulated by alum, whereas gibbsite and boehmite down-regulated gene expression of this proinflammatory cytokine. At the protein expression level, gibbsite hardly induced immunological pathways. Contrarily, boehmite did induce protein expression related to an immune response, although to a lesser extent than alum. Similarly, incubation of monocytes with alum strongly increased IL-1ß secretion by THP-1 cells. These IL-1ß levels were significantly higher than those induced by gibbsite and boehmite.

Differences in monocyte maturation and differentiation were detected at the gene expression level. Both gibbsite and boehmite enhanced gene expression of *TNFα*, a cytokine that is mainly secreted by macrophages.[35] Gibbsite induced gene expression of *CD4*, which is related to monocyte differentiation toward functional mature M2 macrophages.[22] These macrophages are involved in tissue repair upon acute injury, which is induced by vaccination. Boehmite enhanced gene expression of *CSF2*, which is related to the differentiation of monocytes toward proinflammatory M1 macrophages. Alum has been shown to induce monocyte differentiation toward DCs,[36] which was confirmed in this study by the increased *HLA-A* gene expression. Indeed, the interaction of alum with DCs is widely described.[37-39] Thus, boehmite and alum induce monocyte differentiation toward proinflammatory macrophages and DCs,

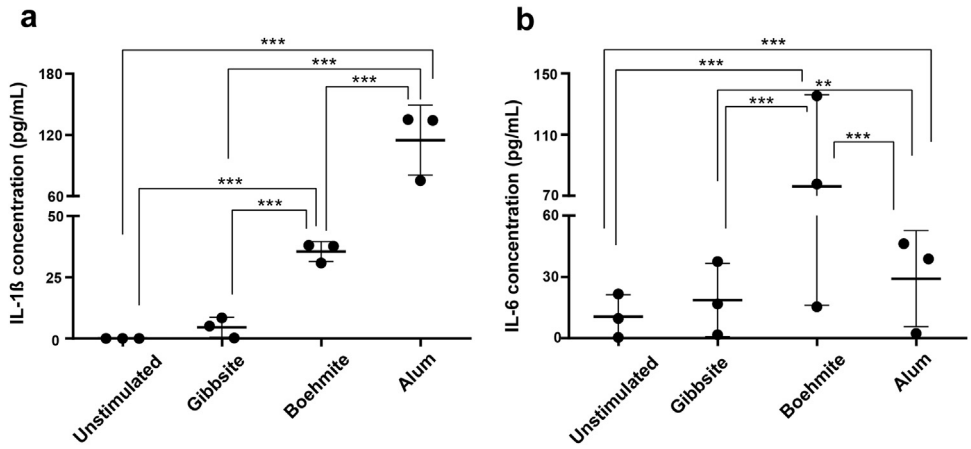

Figure 4. Secretion of IL-1ß (a) and IL-6 (b) after incubation of phorbol myristate acetate–primed THP-1 cells with alum, gibbsite nanoparticles, or boehmite nanoparticles. Data are presented as mean ± SD ($n = 3$). p-Values were determined by using a 2-way ANOVA with multiple comparisons (** = $p < 0.01$, *** = $p < 0.001$).

which are mainly involved in initiating the tissue immune response. Gibbsite induced monocyte differentiation toward functional, noninflammatory macrophages, which are mainly involved in tissue integrity and suppress inflammation.[40] This supports our findings that boehmite mimics alum in the activation of monocytes, albeit with reduced strength at the dose tested.

Gibbsite and boehmite induced fewer stress-related pathways compared to alum as was demonstrated by analysis of protein expression. These pathways may contribute to the adjuvanticity of alum.[41] In addition, homeostatic pathways were mainly upregulated by alum and downregulated by both gibbsite and boehmite. These pathways may play a role in the activation of the immune response by human monocytes.[42] Alternatively, stress and homeostasis might be related to side effects. For example, cell death may lead to the release of cellular material in response to an aluminum-containing adjuvant. An example of such cellular material is uric acid, which causes local inflammation at the site of injection.[43] Because gibbsite and boehmite downregulated homeostatic pathways, these particles may induce an immune response with less side effects than alum. Common limitations of currently used aluminum-based adjuvants include the induction of increased IgE levels, which is related to allergic reactions.[44] In this study, alum induced pathways that are related to allergy, which was not the case for gibbsite nanoparticles and boehmite nanoparticles. However, it is not clear from this study whether this has implications for the use of these particles as vaccine adjuvant.

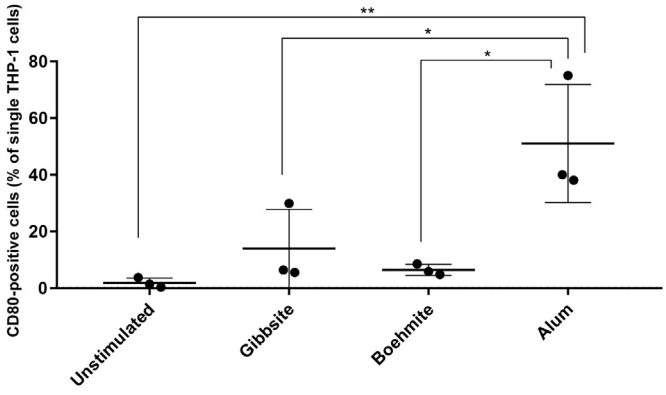

Figure 5. Expression of CD80 on the surface of on phorbol myristate acetate–primed THP-1 cells after incubation with alum, gibbsite nanoparticles, or boehmite nanoparticles. Data are presented as mean ± SD ($n = 3$). p values were determined by using a 2-way ANOVA with multiple comparisons (* = $p < 0.05$, ** = $p < 0.01$).

The zeta potentials of gibbsite and boehmite were comparable in culture medium. Thus, differences in gene and protein expression between alum, gibbsite, and boehmite might be due to the shape and composition. This is also described in the literature. For example, rod-shaped particles were found to be internalized at a higher rate and quantity than spheres and cubes.[45-47] Particle uptake is required for the assembly and activation of the inflammasome via disruption of lysosomal membranes, which in turn induces IL-1ß secretion.[48] Thus, the significant increase in IL-1ß and IL-6 secretion by THP-1 cells on incubation with boehmite might be due to an increased uptake of these particles.

Sun et al. investigated the effects of shape and size of aluminum hydroxide nanoparticles *in vitro* and *in vivo*. They found that the size of aluminum oxyhydroxide nanorods was directly correlated to the activation of the NLRP3 inflammasome in THP-1 cells and in bone marrow–derived dendritic cells (BMDCs), resulting in increased IL-1ß secretion and the expression of the surface markers MHC II, CD80, CD86, and CD40 by BMDCs.[8] By contrast, no effect of the particle size was found on cytokine secretion nor on surface marker expression in the present study. This may be due to the different cell types (BMDCs derived from C57BL/6 mice used by Sun et al. vs. primary human monocytes in this study) and cell culture conditions used, such as different pretreatment of the cells with PMA (300 ng/mL in our study vs. 1 μg/mL by Sun et al.). PMA is used to activate THP-1 cells but can also induce cell differentiation from monocytes into macrophages at higher concentrations. Differentiation into macrophages is characterized by downregulation of CD14.[29] However, the particles used in this study did not alter expression of CD14 (data not shown). In addition, the expression of CD80, CD83, and CD86 was not altered (data not shown), indicating that the monocytes did not differentiate into DCs. In addition, the addition of LPS to induce increased cytokine secretion may have affected cytokine secretion and cell differentiation (2.5 ng/mL in our study vs. 10 ng/mL by Sun et al.). In addition, Sun et al. used Imject alum as a control. This is a mixture of aluminum hydroxide and magnesium hydroxide.[49] It is thus difficult to compare the outcomes of the study of Sun et al. to those of our study.

Seubert et al.[36] found that the expression of MHC II and CD86 on human primary monocytes was increased after incubation with aluminum hydroxide, as demonstrated by an increased mean fluorescence intensity, which was not observed in this study. However, in our study the fluorescence intensity was altered in the presence of the aluminum salt–based particles, making it difficult to distinguish real signal from background noise. In addition, not only monocytes were isolated as in our study, but all PBMCs were

used in the cell culture. Because PBMCs include lymphocytes (T cells, B cells, and NK cells), monocytes, and DCs, it is possible that the interaction between these different cell types influences the expression of surface markers. For example, T cells are needed to increase MHC II on monocytes.[50] This is in agreement with the results of this study, as no increase in MHC II was detected with purified monocytes.

Alum is often described as a Th2-polarizing adjuvant.[50-52] However, this polarization could be related to the research method and species used in the referred studies. For example, alum is a Th2-polarizing adjuvant in mice,[53] but the extent of this effect depends on the mouse strain.[54] Moreover, in humans, a mixed Th1/Th2-polarizing response has been observed.[1,19,55,56] Indications of the activation of monocytes that play a role in the onset of a mixed Th1/Th2 response was also found in this study by the enhanced expression of *IL-4* (Th2-polarizing) and *IFN*γ (Th1-polarizing) on incubation with gibbsite or alum. Boehmite did not induce expression of *IFN*γ and thus may lead to a more Th2-polarizing response. In addition, the innate immune response by an intact organism against complete vaccine formulations may differ from those of isolated immune cells against adjuvants alone. In the present study, the activation of monocytes by colloidal aluminum salt—based vaccine adjuvants was studied in absence of an antigen. However, antigens can alter the innate immune response toward an adjuvant. Hence, the complete vaccine formulation will determine the final response, as described by Kooijman et al.[1,18]

In the present study, we have shown that gibbsite, boehmite, and alum differently activate human monocytes. Hexagonal-shaped gibbsite induced a very limited activation of monocytes, whereas rod-shaped boehmite induced the activation of several pathways that are involved in the onset of an immune response. Hence, rod-shaped aluminum salt—based particles might have stronger cell-activating properties than hexagonal-shaped aluminum salt—based particles. The response of human monocytes toward alum was more intense than the response toward boehmite. However, stress response—related pathways were also much more intensely induced by alum. These pathways are possibly positively related to the activation of an immune response. Alternatively, stress response—related pathways may increase side effects that are currently experienced after immunization with a vaccine containing an aluminum salt—based adjuvant. Apart from alum, boehmite also activated the immune system. Although the activation was less intense compared to alum, the stress-related response induced by boehmite was also much milder. Therefore, boehmite may be a suitable alternative for the currently licensed aluminum hydroxide adjuvant. Future investigations, for example, involving dose-response experiments and a more comprehensive compound library screening (e.g., including other inorganic salts such as aluminum phosphate and calcium phosphate) will be needed to improve our insight into the critical physicochemical properties that influence the immunostimulating effects of particulate aluminum salt—based adjuvants.

Acknowledgments

The authors thank Dedeke Rockx-Brouwer and Lisa Verhagen for their assistance with flow cytometry experiments.

This project was funded by the Ministry of Health, Welfare and Sport, the Netherlands.

References

1. Kooijman S, Brummelman J, van Els C, et al. Novel identified aluminum hydroxide-induced pathways prove monocyte activation and pro-inflammatory preparedness. *J Proteomics*. 2018;175:144-155.
2. Hem JD, Roberson CE. Form and stability of aluminum hydroxide complexes in dilute solution. In: *Geological Survey Water-Supply Paper 1827-A*. Washington, D.C.: United States Government Printing Office; 1967:60.
3. Boraschi D, Italiani P, Palomba R, et al. Nanoparticles and innate immunity: new perspectives on host defence. *Semin Immunol*. 2017;34:33-51.
4. O'Hagan DT, Fox CB. New generation adjuvants–from empiricism to rational design. *Vaccine*. 2015;33(Suppl 2):B14-B20.
5. Li X, Aldayel AM, Cui Z. Aluminum hydroxide nanoparticles show a stronger vaccine adjuvant activity than traditional aluminum hydroxide microparticles. *J Control Release*. 2014;173:148-157.
6. Thakkar SG, Xu H, Li X, Cui Z. Uric acid and the vaccine adjuvant activity of aluminum (oxy)hydroxide nanoparticles. *J Drug Target*. 2018;26:474-480.
7. Benne N, van Duijn J, Kuiper J, Jiskoot W, Slutter B. Orchestrating immune responses: how size, shape and rigidity affect the immunogenicity of particulate vaccines. *J Control Release*. 2016;234:124-134.
8. Sun B, Ji Z, Liao Y-P, et al. Engineering an effective immune adjuvant by designed control of shape and crystallinity of aluminum oxyhydroxide nanoparticles. *ACS Nano*. 2013;7(12):15.
9. Parihar A, Eubank TD, Doseff AI. Monocytes and macrophages regulate immunity through dynamic networks of survival and cell death. *J Innate Immun*. 2010;2(3):204-215.
10. Jakubzick CV, Randolph GJ, Henson PM. Monocyte differentiation and antigen-presenting functions. *Nat Rev Immunol*. 2017;17:349.
11. Oh DY, Dowling DJ, Ahmed S, et al. Adjuvant-induced human monocyte secretome profiles reveal adjuvant- and age-specific protein signatures. *Mol Cell Proteomics*. 2016;15(6):1877-1894.
12. Mosca F, Tritto E, Muzzi A, et al. Molecular and cellular signatures of human vaccine adjuvants. *Proc Natl Acad Sci U S A*. 2008;105(30):6.
13. Johnston CT, Wang SL, Hem SL. Measuring the surface area of aluminum hydroxide adjuvant. *J Pharm Sci*. 2002;91(7):1702-1706.
14. Wierenga AM, Lenstra TAJ, Philipse AP. Aqueous dispersions of colloidal gibbsite platelets - synthesis, characterisation and intrinsic viscosity measurements. *Colloids Surf*. 1998;134:13.
15. Hem SL, Hogenesch H. Relationship between physical and chemical properties of aluminum-containing adjuvants and immunopotentiation. *Expert Rev Vaccin*. 2007;6(5):14.
16. Buining PA, Pathmamanoharan C, Jansen JBH, Lekkerkerker HNW. Preparation of colloidal boehmite needles by hydrothermal treatment of aluminum alkoxide precursors. *J Am Ceram Soc*. 1992;74(6):5.
17. Philipse A. 2 - particulate colloids: aspects of preparation and characterization. In: Lyklema J, ed. *Fundamentals of Interface and Colloid Science*. Amsterdam, The Netherlands: Academic Press; 2005, 2-1-2-71.
18. Kooijman S, Brummelman J, van Els C, et al. Vaccine antigens modulate the innate response of monocytes to Al(OH)3. *PLoS One*. 2018;13(5):e0197885.
19. Moruz L, Pichler P, Stranzl T, Mechtler K, Kall L. Optimized nonlinear gradients for reversed-phase liquid chromatography in shotgun proteomics. *Anal Chem*. 2013;85(16):7777-7785.
20. Harris JR, Soliakov A, Lewis RJ, Depoix F, Watkinson A, Lakey JH. Alhydrogel(R) adjuvant, ultrasonic dispersion and protein binding: a TEM and analytical study. *Micron*. 2012;43(2-3):192-200.
21. Gibbings DJ, Marcet-Palacios M, Sekar Y, Ng MC, Befus AD. CD8 alpha is expressed by human monocytes and enhances Fc gamma R-dependent responses. *BMC Immunol*. 2007;8:12.
22. Zhen A, Krutzik SR, Levin BR, Kasparian S, Zack JA, Kitchen SG. CD4 ligation on human blood monocytes triggers macrophage differentiation and enhances HIV infection. *J Virol*. 2014;88(17):9934-9946.
23. Italiani P, Boraschi D. From monocytes to M1/M2 macrophages: phenotypical vs. functional differentiation. *Front Immunol*. 2014;5:514.
24. Fitzgerald W, Freeman ML, Lederman MM, Vasilieva E, Romero R, Margolis L. A system of cytokines encapsulated in ExtraCellular vesicles. *Sci Rep*. 2018;8(1):8973.
25. Chanput W, Mes JJ, Wichers HJ. THP-1 cell line: an in vitro cell model for immune modulation approach. *Int Immunopharmacol*. 2014;23(1):37-45.
26. Cullen SP, Kearney CJ, Clancy DM, Martin SJ. Diverse activators of the NLRP3 inflammasome promote IL-1beta secretion by Triggering necrosis. *Cell Rep*. 2015;11(10):1535-1548.
27. Hart DN. Dendritic cells: unique leukocyte populations which control the primary immune response. *Blood*. 1997;90(9):3245-3287.
28. Lee J, Tam H, Adler L, Ilstad-Minnihan A, Macaubas C, Mellins ED. The MHC class II antigen presentation pathway in human monocytes differs by subset and is regulated by cytokines. *PLoS One*. 2017;12(8):e0183594.
29. Steinbach F, Thiele B. Phenotypic investigation of mononuclear phagocytes by flow cytometry. *J Immunol Methods*. 1994;174(1):109-122.
30. Chanput W, Peters V, Wichers H. THP-1 and U937 cells. In: Verhoeckx K, Cotter P, López-Expósito I, et al., eds. *The Impact of Food Bioactives on Health: In Vitro and Ex Vivo Models*. Cham: Springer International Publishing; 2015:147-159.
31. Summers KL, Hock BD, McKenzie JL, Hart DN. Phenotypic characterization of five dendritic cell subsets in human tonsils. *Am J Pathol*. 2001;159(1):285-295.
32. Prame Kumar K, Nicholls AJ, Wong CHY. Partners in crime: neutrophils and monocytes/macrophages in inflammation and disease. *Cell Tissue Res*. 2018;371(3):551-565.
33. Zambricki E, Shigeoka A, Kishimoto H, et al. Signaling T-cell survival and death by IL-2 and IL-15. *Am J Transplant*. 2005;5(11):2623-2631.
34. Sinai P, Roybal KT, Wülfing C. Tentative and transient natural killer cell polarization balances the requirements for discriminatory recognition and cytolytic efficacy. *Commun Integr Biol*. 2010;3(6):545-548.

35. Parameswaran N, Patial S. Tumor necrosis factor-α signaling in macrophages. *Crit Rev Eukaryot Gene Expr*. 2010;20(2):87-103.
36. Seubert A, Monaci E, Pizza M, O'Hagan DT, Wack A. The adjuvants aluminum hydroxide and MF59 induce monocyte and granulocyte chemoattractants and enhance monocyte differentiation toward dendritic cells. *J Immunol*. 2008;180(8):5402-5412.
37. Sokolovska A, Hem SL, HogenEsch H. Activation of dendritic cells and induction of CD4(+) T cell differentiation by aluminum-containing adjuvants. *Vaccine*. 2007;25(23):4575-4585.
38. Flach TL, Ng G, Hari A, et al. Alum interaction with dendritic cell membrane lipids is essential for its adjuvanticity. *Nat Med*. 2011;17(4):479-487.
39. Morefield GL, Sokolovska A, Jiang D, HogenEsch H, Robinson JP, Hem SL. Role of aluminum-containing adjuvants in antigen internalization by dendritic cells in vitro. *Vaccine*. 2005;23(13):1588-1595.
40. Gordon S, Taylor PR. Monocyte and macrophage heterogeneity. *Nat Rev Immunol*. 2005;5(12):953-964.
41. Wang Y, Rahman D, Lehner T. A comparative study of stress-mediated immunological functions with the adjuvanticity of alum. *J Biol Chem*. 2012;287(21):17152-17160.
42. Pearce EJ, Everts B. Dendritic cell metabolism. *Nat Rev Immunol*. 2015;15(1):18-29.
43. Álvarez-Lario B, MacArrón-Vicente J. Is there anything good in uric acid? *QJM*. 2011;104(12):1015-1024.
44. Terhune TD, Deth RC. Aluminum adjuvant-containing vaccines in the context of the hygiene hypothesis: a risk factor for Eosinophilia and allergy in a genetically susceptible subpopulation? *Int J Environ Res Public Health*. 2018;15(5):901.
45. Niikura K, Matsunaga T, Suzuki T, et al. Gold nanoparticles as vaccine platform - influence of size and shape on immunological responses in vitro and in vivo. *ACS Nano*. 2013;7(5):13.
46. Zheng M, Yu J. The effect of particle shape and size on cellular uptake. *Drug Deliv Transl Res*. 2016;6(1):67-72.
47. Gratton SEA, Ropp PA, Pohlhaus PD, et al. The effect of particle design on cellular internatization pathways. *Proc Natl Acad Sci U S A*. 2008;105(33):6.
48. Harte C, Gorman AL, McCluskey S, et al. Alum activates the bovine NLRP3 inflammasome. *Front Immunol*. 2017;8:1494.
49. Hem SL, Johnston CT, HogenEsch H. Imject Alum is not aluminum hydroxide adjuvant or aluminum phosphate adjuvant. *Vaccine*. 2007;25(27):4985-4986.
50. Ulanova M, Tarkowski A, Hahn-Zoric M, Hanson LA. The common vaccine adjuvant aluminum hydroxide up-regulates accessory properties of human monocytes via an interleukin-4-dependent mechanism. *Infect Immun*. 2001;69(2):1151-1159.
51. Miki H, Nakahashi-Oda C, Sumida T, Shibuya A. Involvement of CD300a phosphatidylserine Immunoreceptor in aluminum salt adjuvant−induced Th2 responses. *J Immunol*. 2015;194:5069-5076.
52. McKee AS, Munks MW, MacLeod MK, et al. Alum induces innate immune responses through macrophage and mast cell sensors, but these sensors are not required for alum to act as an adjuvant for specific immunity. *J Immunol*. 2009;183(7):4403-4414.
53. Knudsen NP, Olsen A, Buonsanti C, et al. Different human vaccine adjuvants promote distinct antigen-independent immunological signatures tailored to different pathogens. *Sci Rep*. 2016;6:19570.
54. Zeng M, Nouri-Shirazi E, Guinet E, Nouri-Shirazi M. The genetic background influences the cellular and humoral immune responses to vaccines. *Clin Exp Immunol*. 2016;186:190-204.
55. Hogenesch H. Mechanism of immunopotentiation and safety of aluminum adjuvants. *Front Immunol*. 2012;3:406.
56. He P, Zou Y, Hu Z. Advances in aluminum hydroxide-based adjuvant research and its mechanism. *Hum Vaccin Immunother*. 2015;11(2):477-488.